JOURNAL OF ADVANCED DIELECTRICS
Vol. 8, No. 1 (2018) 1850004 (8 pages)

DOI: 10.1142/S2010135X18500042

World Scientific
www.worldscientific.com

Processing and characterization of lead-free ceramics on the base of sodium–potassium niobate

E. D. Politova*,¶, N. V. Golubko*, G. M. Kaleva*, A. V. Mosunov*, N. V. Sadovskaya*, S. Yu. Stefanovich*, D. A. Kiselev†,‡, A. M. Kislyuk† and P. K. Panda§

*L. Ya.Karpov Institute of Physical Chemistry
Vorontsovo Pole, 10, Moscow 105064, Russia

†National University of Science and Technology "MISiS"
Leninskii pr. 4, Moscow 119991, Russia

‡Kotelnikov Institute of Radio Engineering and Electronics
Russian Academy of Sciences (Fryazino Branch)
pl. Vvedenskogo 1, Fryazino, Moscow Region 141190, Russia

§National Aerospace Laboratories
Kodihalli, Bangalore 560017, India

¶politova@cc.nifhi.ac.ru

Received 14 December 2017; Revised 19 January 2018; Accepted 29 January 2018; Published 27 February 2018

Lead-free sodium–potassium niobate-based piezoelectric materials are most intensively studied in order to replace the widely used Pb-based ones. In this work, the effects of modification of compositions by donor and acceptor dopants in the A- and B-sites of perovskite lattice on structure, dielectric, ferroelectric, and piezoelectric properties of ceramics from Morphotropic Phase Boundary in the $(1-x)(K_{0.5}Na_{0.5})NbO_3$–$xBaTiO_3$ system and in compositions with $x = 0.05$ and 0.06 additionally doped by Ni^{3+} cations have been studied.

Keywords: $(Ka_{0.5}Na_{0.5})NbO_3$; $BaTiO_3$; perovskite structure; solid solutions; phase transitions; dielectric; ferroelectric; piezoelectric properties.

1. Introduction

The development of piezoelectric materials without toxic lead comprises an important task from the environmental point of view.[1–18] Among them, potassium–sodium niobate (K,Na)NbO_3 (KNN) is regarded the most promising material.[1,7,8,11,19–23] Piezoelectric properties of materials based on KNN are determined by the ratio of orthorhombic (O) and tetragonal (T) phases. Accordingly, one of the strategies for achieving a larger piezoelectric response is to ensure a change in the compositions based on KNN in such a way that the transition temperature from O to T phase should be close to room temperature. In addition, to the formation of functional properties of piezoceramics, substitutions in A- and B- sites, methods of preparation and polarization of ceramics, the presence of oxygen vacancies make an important contribution.

It should be noted that in spite of intensive research and progress made in the studies of Pb-free compositions, their developments are still far from achieving the goal of creating lead-free family exhibiting a wide range of properties comparable with those of PZT.

Incorporation of donor and/or acceptor dopants into the A- and B-sites of perovskite lattice will influence "softening" and "hardening" effects, mechanical quality factor, and dielectric losses. Additionally, aliovalent substitutions in A- and B-sites stimulate relaxor properties of ceramics expecting the enhancement of piezoelectric properties of the material.

In this work, the effects of modification of compositions by donor (Ba^{2+}) and acceptor dopants (Ni^{3+}) in the A- and B-sites of perovskite lattice on structure, dielectric and ferroelectric properties of ceramics from Morphotropic Phase Boundary (MPB) in the $(K_{0.5}Na_{0.5})NbO_3$–$BaTiO_3$ (I) ($x =$ 0–0.08) and in the $[(K_{0.5}Na_{0.5})_{1-x}Ba_x][(Nb_{1-x}Ti_x)_{1-y}Ni_y]O_3$ (II) ($x = 0.05, 0.06$; $y = 0.01, 0.03, 0.05$) systems have been studied.

2. Experimental

Ceramic samples in the $(1-x)(K_{0.5}Na_{0.5})NbO_3$–$xBaTiO_3$ (I) system with $x =$ 0–0.08 were prepared by the solid state reaction method at $T_1 = 1073$ K (6 h), $T_2 = 1223$ K (6 h)

(calcinations), $T_3 = 1423$ K (2 h) (sintering). The samples $[(K_{0.5}Na_{0.5})_{1-x}Ba_x][(Nb_{1-x}Ti_x)_{1-y}Ni_y]O_3$ (II) with $x = 0.05$, 0.06; $y = 0.01$, 0.03, 0.05 were obtained at $T_1 = 1073$ K (6 h), $T_2 = 1423$ K (2 h). Sodium carbonate Na_2CO_3, potassium carbonate K_2CO_3, barium carbonate $BaCO_3$, Nb_2O_5, Ni_2O_3, and TiO_2 oxides (all of "pure" grade) were used as starting materials. Before synthesis, all carbonates were dried at 873 K in order to remove the absorbed water and carbon dioxide.

The samples were characterized by the X-ray diffraction (DRON-3M, Cu-K_α radiation with wavelength $\lambda =$ 1.5405 A, in the 2θ range of 5–80°, with step-scan interval and step-scan time of 0.05° and 1 s, respectively). The Second Harmonic Generation (SHG, Nd:YAG laser, $\lambda = 1.064\ \mu$m in the reflection) method was used to evaluate the spontaneous polarization of the samples. Dielectric measurements were performed on the samples with fired silver electrodes on heating (10 K/min.) and cooling in the temperature interval of 300–1000 K, in the frequency range of 100 Hz–1 MHz using Agilent 4284 A (1 V). Microstructure of the samples was examined by the Scanning Electron Microscopy (SEM) method (JEOL YSM-7401F with a JEOL JED-2300 energy dispersive X-ray spectrometer system).

The surface morphology and as-grown domain structure of the samples were characterized by piezoresponse force microscopy (PFM) method using a commercial scanning probe microscope MFP-3D (Asylum Research, USA) with Asyelec Ti/Ir-coated conductive probes (Asyelec-02, Asylum Research, USA). Vertical PFM (VPFM) images of the ceramic samples were recorded by applying an AC voltage of $V_{ac} = 3$ V with a frequency of 900 kHz to the cantilever (close to contact cantilever resonance frequency). During the piezoelectric hysteresis loop measurements (remnant loops), an AC voltage was superimposed onto a triangular square-stepping wave ($f = 0.5$ Hz, writing time = read time = 25 ms, bias window up to ±50 V). For the estimation of the piezoelectric constants (effective d_{33}), the deflections and vibration sensitivity of the cantilever alignment were calibrated by GetReal procedure in IgorPro software (Asylum Research, USA). For PFM characterization, the samples were carefully polished using polycrystalline diamond with different sizes. The root mean square roughness of all the samples was less than 10 nm.

3. Results and Discussion

In (I) and (II) systems, the samples with perovskite structure were prepared (Figs. 1(a) and 1(b)). Small peaks of admixture phase $K_2Nb_8O_{21}$ were observed in the X-ray diffraction patterns.

Depending on the A- and B-cation substitutions, changes in the structure from tetragonal to orthorhombic ones were observed in the samples (I) (Fig. 2(a)). However, the samples (II) all revealed tetragonal structure (Fig. 2(b)). A slight increase in the unit cell parameters observed for the KNN-BT ceramics correlates well with substitution of cations with smaller ionic radii (K^+ and Na^+) by larger Ba^{2+}-cations. The introduction of small amount of Ni^{3+} cations practically does not influence the unit cell volume of ceramics II. A slight increase in the unit cell parameters of the Ni-doped ceramics may be explained by the losses of the A-site cations due to the reduction of B cations (Fig. 2(b)).

The microstructure of the samples is sensitive to substitutions and to sintering conditions as well. With increasing the sintering temperature, the enlargement of mean size of grains was observed (Figs. 3(a) and 3(b)). However, the increasing concentration of the barium titanate stimulates a

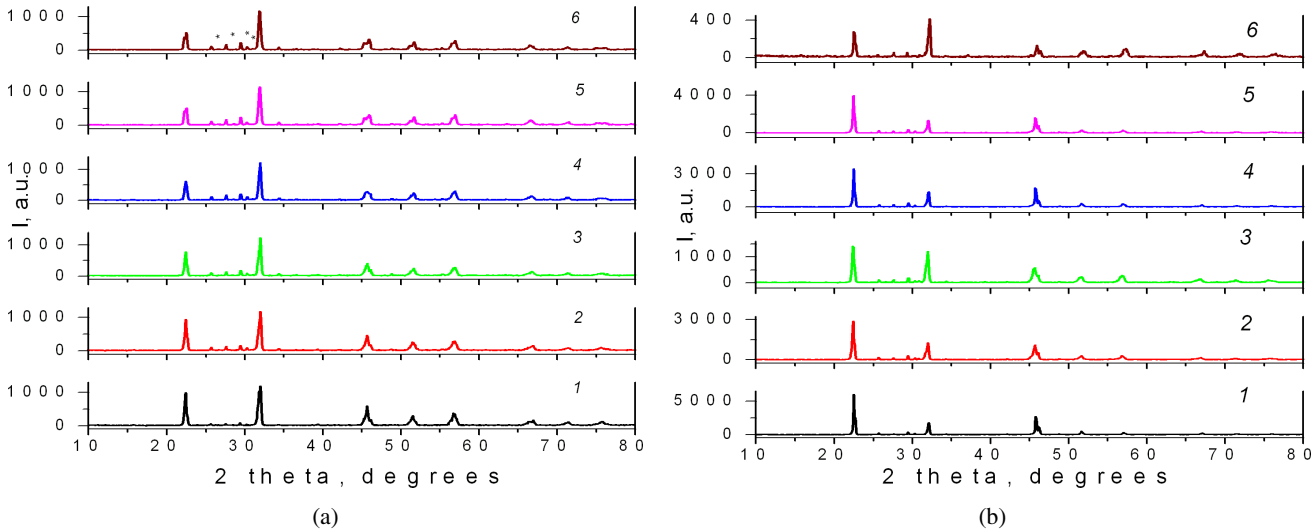

Fig. 1. The X-ray diffraction patterns of the samples (a) $(1-x)(K_{0.5}Na_{0.5})NbO_3$–$xBaTiO_3$ with $x = 0$–0.08 prepared by the solid state reaction method at $T_1 = 1073$ K (6 h), $T_2 = 1223$ K (6 h), $T_3 = 1423$ K (2 h) and of the samples (b) $[(K_{0.5}Na_{0.5})_{1-x}Ba_x][(Nb_{1-x}Ti_x)_{1-y}Ni_y]O_3$ (II) with $x = 0.05$, 0.06; $y = 0.01$, 0.03, 0.05 sintered at $T_2 = 1423$ K (2 h).

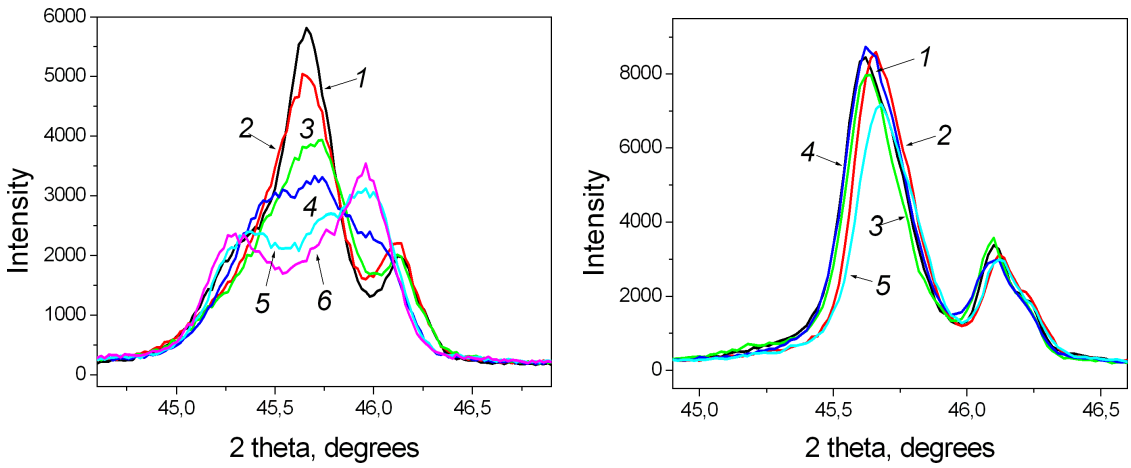

Fig. 2. Parts of the X-ray diffraction patterns showing peaks with $h^2 + k^2 + l^2 = 4$ for the (a) $(1 - x)(K_{0.5}Na_{0.5})NbO_3$–$xBaTiO_3$ and (b) $[(K_{0.5}Na_{0.5})_{1-x}Ba_x][(Nb_{1-x}Ti_x)_{1-y}Ni_y]O_3$ samples.

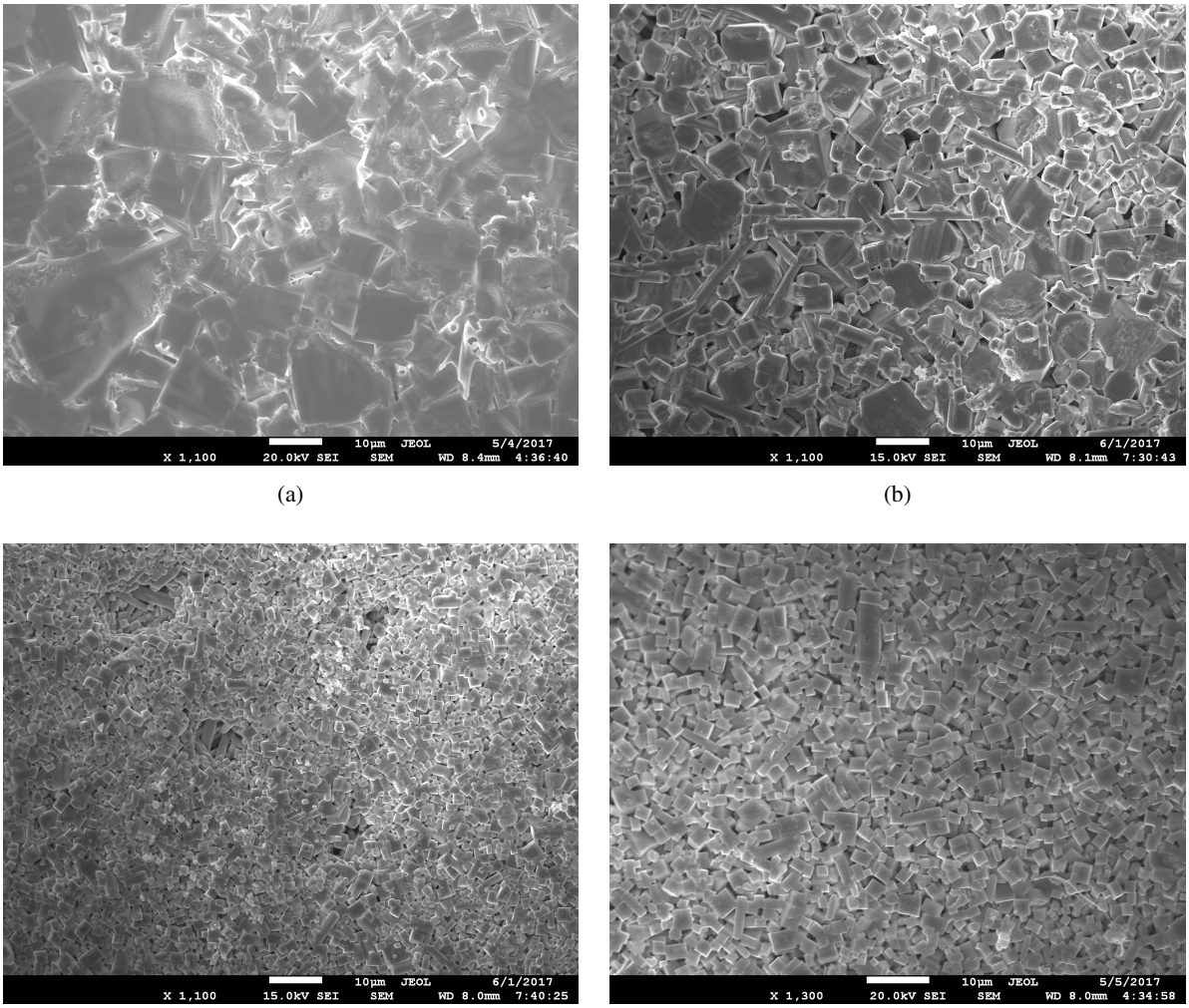

Fig. 3. Microstructure of the surface of the $(1 - x)(K_{0.5}Na_{0.5})NbO_3$–$xBaTiO_3$ samples with (a,b) $x = 0.02$, (c) 0.06, (d) 0.08 sintered at (a,c,d) $T = 1423$ K and at (b) $T = 1413$ K.

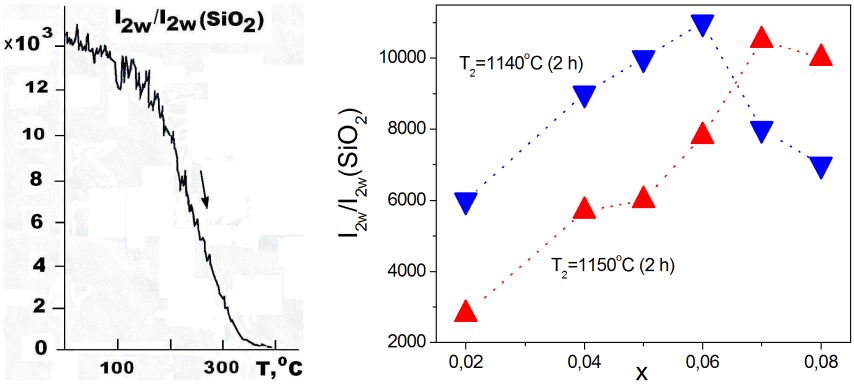

(a) (b)

Fig. 4. (a) Temperature dependence of the SHG signal intensity for the sample (I) with $x = 0.08$ sintered at $T_2 = 1423$ K (2 h). (b) Concentration dependence of the SHG signal intensity for the sample (I) sintered at different temperatures.

decrease in the size of grains with cubic form (Figs. 3(c) and 3(d)).

It was confirmed that all samples belonged to the polar structures indicate their ferroelectric properties. Spontaneous polarization value *Ps* was estimated using the SHG method taking into account that the relative intensity of the SHG signal $q \sim I_{2w}/I_{2w}$ (SiO_2) was related to the spontaneous polarization *Ps* as $q \sim Ps^{0.5}$.[24] At the room temperature, all samples (I) produce high SHG signal $q = 2000$–$13{,}000$ corresponding to a noncentrosymmetric oxide material. Increase in the SHG signal q value which is proportional to the spontaneous polarization value was proved for modified KNN-BT ceramics with $y = 0.02$–0.06 indicating the strengthening of ferroelectric properties in modified compositions (I) (Fig. 4).

Initial KNN samples are characterized by two phase transitions, with the orthorhombic phase transforming to the tetragonal one and then to paraelectric one.[18–25] Accordingly, ferroelectric phase transitions marked by steps near ~400 K and by pronounce maxima at ~600 K were revealed in the dielectric permittivity versus temperature curves of the compositions studied. A slight increase in temperatures of both phase transitions was observed in ceramic solid solutions (Figs. 5(a) and 5(b)).

At the room temperature, nonmonotonous changes of the dielectric parameters ε_{rt} and $\tan\delta_{rt}$ and *Ps* values were observed in modified KNN-based compositions, thus confirming their prospects for new lead-free materials development.

Simultaneous topography and VPFM images (Figs. 6(1a)–(5a) and 6(1b)–(5b)) show that the imaged pattern is entirely due to the piezoresponse and not cross-coupling to the surface topography. In the VPFM images, bright contrast areas represented domains with downward polarization orientation, while dark contrast represented the opposite case. Complex domain structure consisting of multiple domain patterns was found for all investigated ceramic samples (Figs. 6(1b)–(5b) and 7). At the same time, a brownish, background contrast corresponds to zero vertical

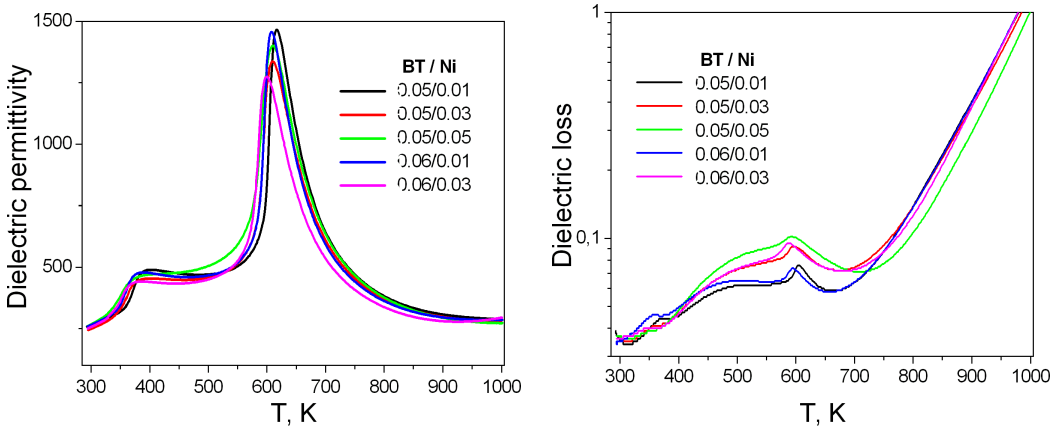

(a) (b)

Fig. 5. Temperature dependences of (a,c,e) dielectric permittivity $\varepsilon(T)$ and (b,d,f) dielectric loss $\tan\delta(T)$ of the samples $[(K_{0.5}Na_{0.5})_{1-x}Ba_x][(Nb_{1-x}Ti_x)_{1-y}Ni_y]O_3$ with (a,b) $x = 0.05$ and 0.06, $y = 0.01$, 0.03, 0.05, with (e,f) $x = 0.05$, $y = 0.01$ and samples $(1-x)(K_{0.5}Na_{0.5})NbO_3$–$x$ $BaTiO_3$ with (c,d) $x = 0.04$ sintered at $T_3 = 1423$ K (2 h) measured at frequencies (a,b) $f = 1$ MHz and at (c–f) $f = 100$ Hz–1 MHz.

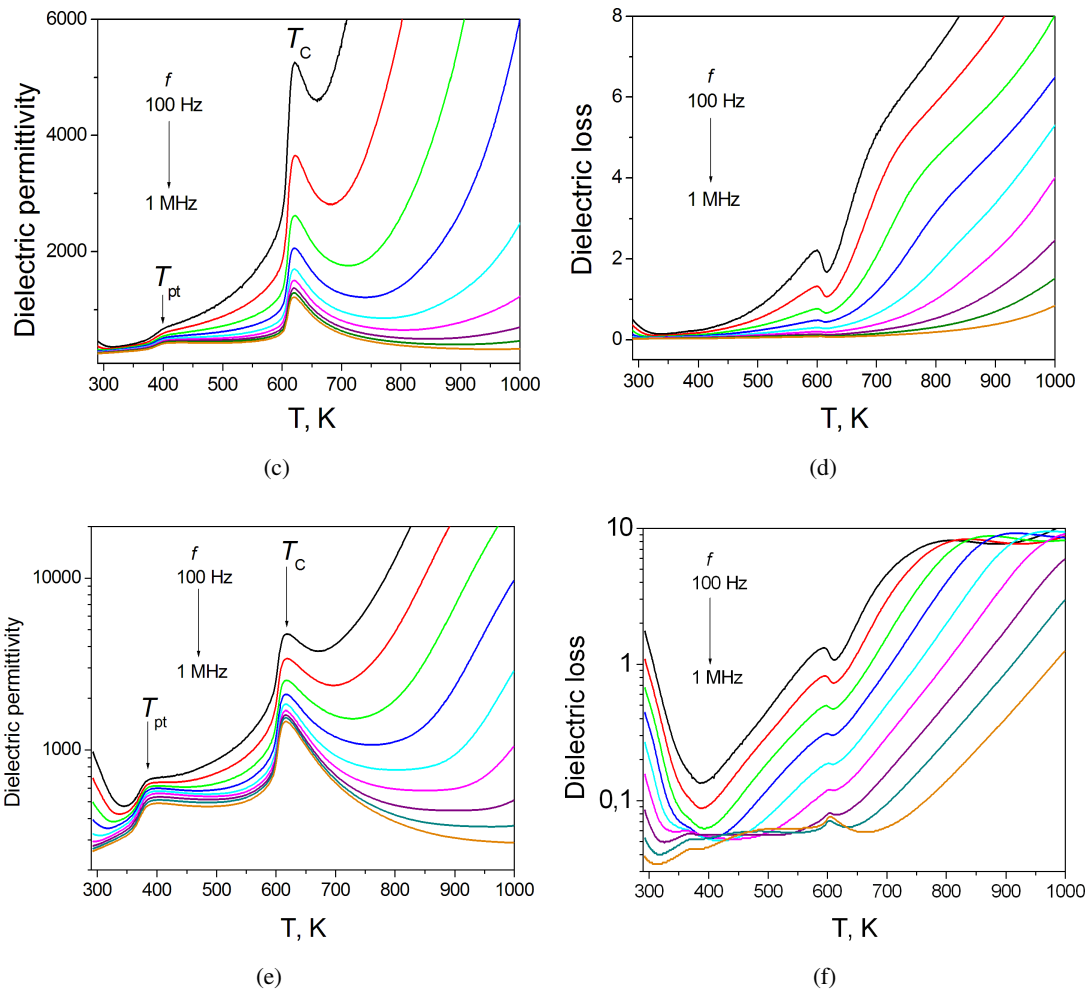

Fig. 5. (*Continued*)

piezoresponse and is attributed to factors: (i) lateral polarization orientation of the domains or (ii) piezoelectrically inactive grains. The latter is less preferable, as will be shown below.

To study the polarization switching inside grains, we have measured local piezoresponse hysteresis loops. Two points on ceramics were chosen to measure the local piezoresponse at the selected localized regions.

Region (1) is located at the area which shows large domain contrast while region (2) is an area which has a weak piezoresponse signal in VPFM image. Figures 6(1c)–(5c) and 7 demonstrate the well-shaped effective d_{33} hysteresis loops for the KNN-doped ceramics.

As can be seen from hysteresis loops, the value of the maximal effective piezoelectric coefficient strongly depends on the measurement location. The grains with high VPFM response (region (1)) exhibit larger value of the effective d_{33} at maximum poled voltage than grains with weak piezoresponse. This indicates that the ferroelectric polarization of these grains may be mainly oriented parallel to the sample surface. On the other hand, in case of location (2), the hysteresis loops are off-centered toward the negative direction, indicating large polarization imprint. The d_{33} hysteresis loops measured at region (1) also follow a similar trend.

For all ceramic samples, the loops measured on region (1) are often distorted, that is, shifted toward either positive or negative bias voltage. Such shift indicates to the presence of internal bias fields stabilizing an energetically more favorable orientation of the polarization along their directions, and resulting in an asymmetry of the switching process.[25,26] On the other hand, the value of effective d_{33} at +50 V is lower than that recorded at −50 V. Observations of similarly distorted and asymmetrical butterfly hysteresis loops are commonly reported for ceramic samples.[27,28] The presence of non-180° domains inside the grains may also explain why the strain caused by the positive voltage differs from that of the negative voltage. Finally, effective d_{33} piezoelectric coefficient values reach 300 pm/V in the KNN-BT system and 200 pm/V in the KNN-BT samples additionally doped by Ni^{3+} cations.

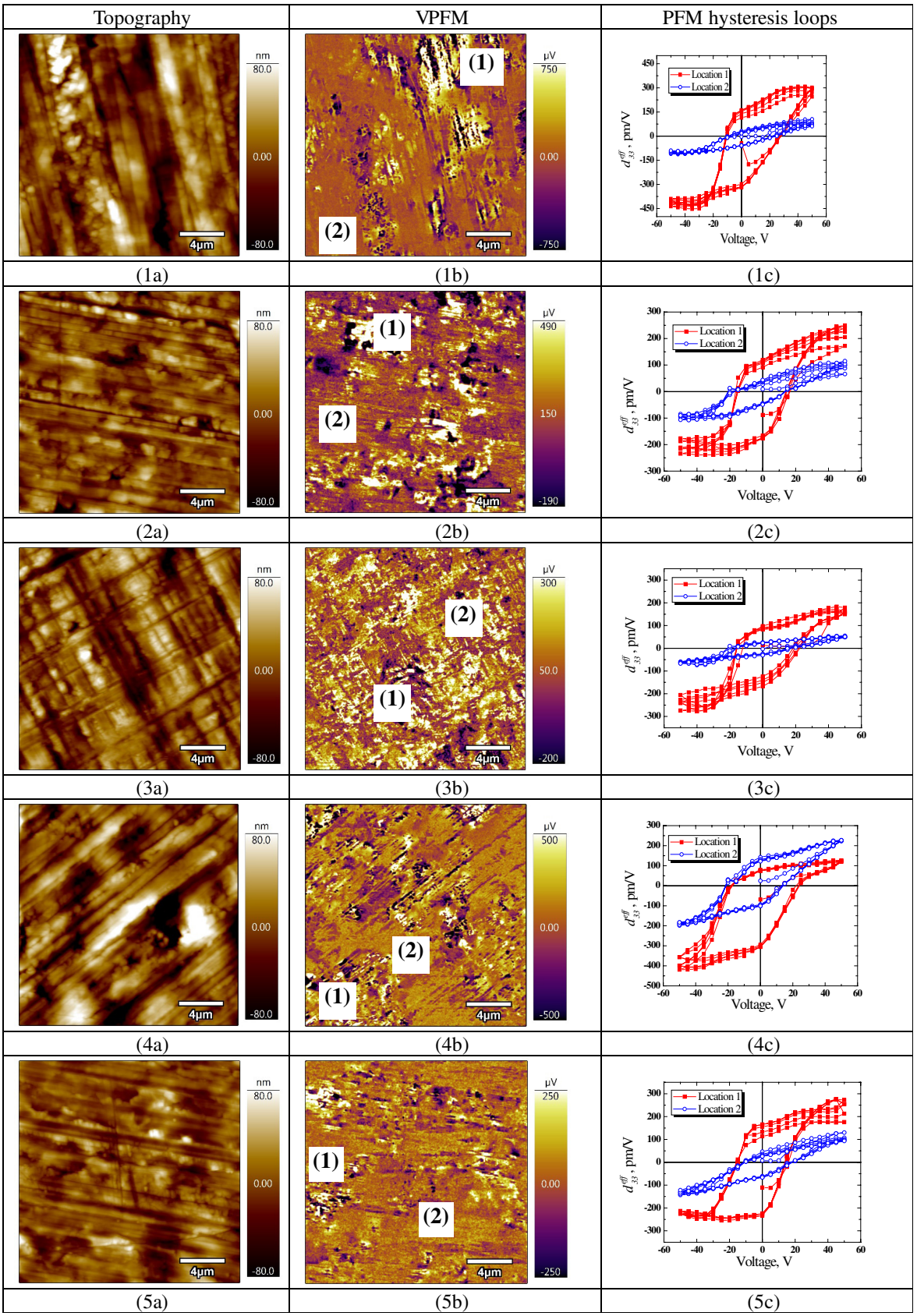

Fig. 6. (1a)–(5a) Topography of the samples (I) with $x = 0.05$ (1) and $x = 0.06$ (2) and samples (II) with $x = 0.05$, $y = 0.05$ (3), 0.01 (4), 0.03 (5) (after polishing); (1b)–(5b) VPFM image; (1c)–(5c) local PFM hysteresis loops from regions marked (1) and (2) in VPFM images.

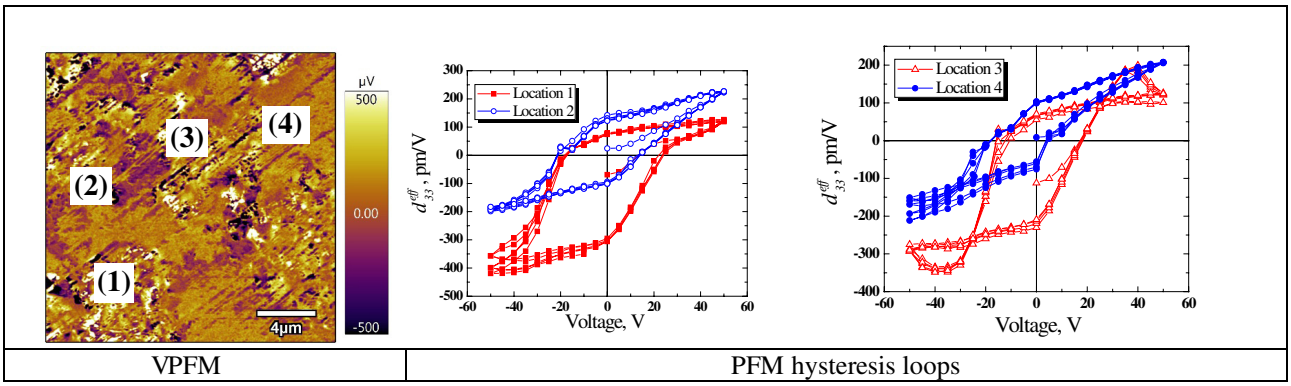

Fig. 7. VPFM image of the sample (II) with $x = 0.05, y = 0.01$ (after polishing); local PFM hysteresis loops from regions marked by (1)–(4) in the VPFM image.

4. Conclusions

Structure parameters, microstructure, dielectric and ferroelectric properties of ceramics in the $(1-x)(K_{0.5}Na_{0.5})NbO_3$–$x$ $BaTiO_3$ and $[(K_{0.5}Na_{0.5})_{1-x}Ba_x][(Nb_{1-x}Ti_x)_{1-y}Ni_y]O_3$ systems obtained were studied. Depending on the composition and sintering conditions, changes in the unit cell volume were observed. An increase in the $BaTiO_3$ and Ni^{3+} cations content leads to slight decrease in the T_m and T_{pt} values. Nonmonotonous changes of dielectric parameters and spontaneous polarization were observed that favor to the improvement of their functional properties. PFM was used to study the as-grown domain structure in lead-free ceramics in (I) and (II) systems. The hysteresis behavior of the piezoresponse of the ceramic confirmed their ferroelectric switching behavior. High values of the effective d_{33} piezoelectric coefficient were measured in the samples studied.

Acknowledgment

The work was supported by the Russian Foundation for Basic Research (Project 16-53-48009).

References

[1]E. Cross, Materials science-lead-free at last, *Nature* **432**, 24 (2004).
[2]Y. Saito, H. Takao, T. Tani, T. Nonoyama, K. Takatori, T. Homma, T. Nagaya and M. Nakamura, Lead-free piezoceramics, *Nature* **432**, 84 (2004).
[3]H.-Y. Park, C.-W. Ahn, H.-C. Song, J.-H. Lee and S. Nahma, Microstructure and piezoelectric properties of $0.95Na_{0.5}K_{0.5}NbO_3$–$0.05BaTiO_3$ ceramics, *Appl. Phys. Lett.* **89**, 062906, 2006.
[4]S. Priya, Advances in energy harvesting using low profile piezoelectric transducers, *J. Electroceram.* **19**, 165 (2007).
[5]S. J. Zhang, R. Xia and R. T. Shrout, Lead-free piezoelectric ceramics: Alternatives for PZT? *J. Electroceram.* **19**, 251 (2007).
[6]T. Takenaka, H. Nagata and Y. Hiruma, Current developments and prospective of lead-free piezoelectric ceramics, *Jpn. J. Appl. Phys.* **47**, 3787 (2008).
[7]P. K. Panda, Review: Environmental friendly lead-free piezoelectric materials, *J. Mater. Sci.* **44**, 5049 (2009).
[8]Y.-J. Dai, X.-W. Zhang and K.-P. Chen, Morphotropic phase boundary and electrical properties of $K_{1-x}Na_xNbO_3$ lead-free ceramics, *Appl. Phys. Lett.* **94**, 042905 (2009).
[9]D. Damjanovich, N. Klein, J. Li and V. Porokhonskyy, What can be expected from lead-free piezoelectric materials? *Funct. Mater. Lett.* **3**, 5 (2010).
[10]D. Q. Xiao, Progresses and further considerations on the research of perovskite lead-free piezoelectric ceramics, *J. Adv. Dielectr.* **1**, 33 (2011).
[11]Y. Q. Lu and Y. X. Li, A review on lead-free piezoelectric ceramics studied in China, *J. Adv. Dielectr.* **1**, 269 (2011).
[12]J. Fang, X. Wang, R. Zuo, Z. Tian, C. Zhong and L. Li, Narrow sintering temperature window for $(K,Na)NbO_3$-based lead-free piezoceramics caused by compositional segregation, *Phys. Status Solidi A* **208**, 791 (2011).
[13]J. L. Hyeong and Z. H. Shujun, Perovskite lead-free piezoelectric ceramics, *Lead-Free Piezoelectrics*, eds. S. Priya and S. Nahm (Springer, New York, 2012), pp. 291–309.
[14]K. Wang and J.-F. Li, $(K,Na)NbO_3$-based lead-free piezoceramics: Phase transition, sintering and property enhancement, *J. Adv. Ceram.* **1**, 24 (2012).
[15]I. Coondoo, N. Panwar and A. Kholkin, Lead-free piezoelectrics: Current status and perspectives, *J. Adv. Dielectr.* **3**, 1330002 (2013).
[16]P. K. Panda and B. Sahoo, PZT to lead-free piezo ceramics, *Ferroelectrics* **474**, 128 (2015).
[17]C. H. Hong, H. P. Kim, B. Y. Choi, H. S. Han, J. S. Son, C. W. Ahn and W. Jo, Lead-free piezoceramics. Where to move on? *J. Materiomics* **2**, 1 (2016).
[18]R. Zuo, J. Roedel, R. Chen and L. Li, Sintering and electrical properties of lead-free $Na_{0.5}K_{0.5}NbO_3$ piezoelectric ceramics, *J. Am. Ceram. Soc.* **89**, 2010 (2006).
[19]S. Zhang, R. Xia and T. R. Shrout, Modified $(K_{0.5}Na_{0.5})NbO_3$ based lead-free piezoelectrics with broad temperature usage range, *Appl. Phys. Lett.* **91**, 132913 (2007).
[20]J. Tellier, B. Malic, B. Dkhil, D. Jenko, J. Cilensek and M. Kosec, Crystal structure and phase transitions of sodium potassium niobate perovskites, *Solid State Sci.* **11**, 320 (2009).
[21]J.-F. Li, K. Wang, F.-Y. Zhu, L.-Q. Cheng and F.-Z. Yao, $(K,Na)NbO_3$-based lead-free piezoceramics: Fundamental aspects, processing technologies, and remaining challenges, *J. Am. Ceram. Soc.* **96**, 3677 (2013).

[22]J. G. Wu, D. Q. Xiao and J. G. Zhu, Potassium–sodium niobate lead-free piezoelectric materials: Past, present, and future of phase boundaries, *Chem. Rev.* **115**, 2559 (2015).
[23]B. Malič, J. Koruza, J. Hreščak, J. Bernard, K. Wang, J. G. Fisher and A. Benčan, Sintering of lead-free piezoelectric sodium potassium niobate ceramics, *Materials* **12**, 8117 (2015).
[24]E. D. Politova, G. M. Kaleva, N. V. Golubko, A. V. Mosunov, A. S. Akinfiev, S. Y. Stefanovich and E. A. Fortalnova, Influence of NaCl/LiF additives on structure, microstructure and phase transitions of $(K_{0.5}Na_{0.5})NbO_3$ ceramics, *Ferroelectrics* **489**, 147 (2015).
[25]S. Jesse, A. P. Baddorf and S. V. Kalinin, Switching spectroscopy piezoresponse force microscopy of ferroelectric materials, *Appl. Phys. Lett.* **88**, 062908 (2006).
[26]H. Trivedi *et al.*, Local manifestations of a static magnetoelectric effect in nanostructured $BaTiO_3$–$BaFe_{12}O_9$ composite multiferroics, *Nanoscale* **7**, 4489 (2015).
[27]D. Damjanovic, *Hysteresis in Piezoelectric and Ferroelectric Materials*, eds. I. Mayergoyz and G. Bertotti (Elsevier, New York, 2005), pp. 337–465.
[28]D. E. Dausch, Asymmetric 90° domain switching in rainbow actuators, *Ferroelectrics* **210**, 31 (1998).